ELSEVIER

Journal of Photochemistry and Photobiology A: Chemistry 154 (2002) 23–32

Journal of Photochemistry and Photobiology A:Chemistry

www.elsevier.com/locate/jphotochem

Nodal-plane model for excited-state intramolecular proton transfer of *o*-hydroxybenzaldehyde: substituent effect

Shin-ichi Nagaoka [a,*], Arinobu Nakamura [a], Umpei Nagashima [b]

[a] *Chemistry Group, Department of Fundamental Material Science, Faculty of Science, Ehime University, Matsuyama 790-8577, Japan*
[b] *Grid Technology Research Center, National Institute of Advanced Industrial Science and Technology, 1-1-1 Umezono, Tsukuba 305-8568, Japan*

Received 19 February 2002; received in revised form 9 May 2002; accepted 28 May 2002

Abstract

The excited-state intramolecular proton transfer (ESIPT) of *o*-hydroxybenzaldehyde (OHBA) and related molecules in solution has been studied by emission spectroscopy. The substituent effects on the fluorescence quantum yield for the lowest excited $^1(\pi,\pi^*)$ state can be explained by considering the nodal pattern of the wave function along with the delocalization of the π electrons in the excited state. The substituent effect in 5-substituted salicylaldehydes is much less than that in *o*-(substituted-formyl)phenols.

Keywords: Excited-state intramolecular proton transfer (ESIPT); *o*-Hydroxybenzaldehyde; Fluorescence quantum yield; Nodal-plane model; Substituent effect

1. Introduction

Much attention has been directed, from both experimental and theoretical viewpoints, toward the excited-state intramolecular proton transfer (ESIPT) of hydrogen-bonded molecules [1–12]. ESIPT is a very simple chemical process readily accessible for both accurate measurement and quantitative theoretical analysis. The study of ESIPT is at the forefront of the revolution in understanding chemical reactions at the molecular level.

We have investigated the dynamic processes in the low-lying excited states of *o*-hydroxybenzaldehyde (OHBA) and its related molecules (OHBAs) by using spectroscopic and computational methods [13–29]. We constructed a simple theoretical model of ESIPT in OHBAs, based on the nodal pattern of the wave function [17,18]. Although this nodal-plane model is qualitative, it allows us to immediately recognize the important features of ESIPT, and it provides useful information about the reaction mechanisms of ESIPT. Our model is applicable to various photochemical reactions occurring at various excited states of various molecules [30,31].

Many chemists have cited our nodal-plane model [5–12,32–59], and recognized the usefulness of our explanation as mentioned below. Recent reviews [5,8–11,32] and special issues [6,7,12] have extensively discussed it. The mechanism of ESIPT for the lowest excited singlet state (S_1 state) of 2,5-bis(benzoxazolyl)hydroquinone, in which only one proton is transferred even though the molecule has two equivalent intramolecular-hydrogen-bonds, has been explained in terms of our nodal-plane model [33,36,39]. The absence of proton transfer in the S_1 state of 2-hydroxyquinoline has been understood in terms of nodal-plane analysis of the wave function [38]. The ESIPT's of methylsalicylate (MS) [40], 2-hydroxy-3-naphthoate [42], salicylic acid (SA) [45] and hydroxyanthraquinones [48] have been interpreted with the nodal-plane model. Our model has also been used to analyze proton-transfer processes in thermochromic crystalline salicylidenanilines [47]. The substituent effect in ESIPT of 1-hydroxy-2-acetonaphthone and related molecules has also supported our view [50]. For not only ESIPTs of aromatic anils [52] but also the excited-state intermolecular proton transfer of 7-azaindole dimer [54,55], the excited-state dependence of reactivity has been understood in terms of nodal-plane analysis of the wave function. Our model has also been applied to the ground-state proton transfer of salicylate anion [56]. Our explanation has also been used widely to interpret various photoreactions, in addition to proton transfer, such as the photorearrangement of *o*-vinyl diaryl ethers [57,58] and the photoisomerization of retinal chromophore in bacteriorhodopsin [59].

* Corresponding author. Present addresses: Institute for Molecular Science, Okazaki 444-8585, Japan; Also at: Institute for Solid State Physics, University of Tokyo, Kashiwanoha, Kashiwa 277-8581, Japan; and Hiroshima Synchrotron Radiation Center, Hiroshima University, Higashi-Hiroshima 739-8526, Japan. Tel.: +81-89-927-9592; fax: +81-89-927-9590.
E-mail address: nagaoka@ehimegw.dpc.ehime-u.ac.jp (S. Nagaoka).

1010-6030/02/$ – see front matter
PII: S1010-6030(02)00305-2

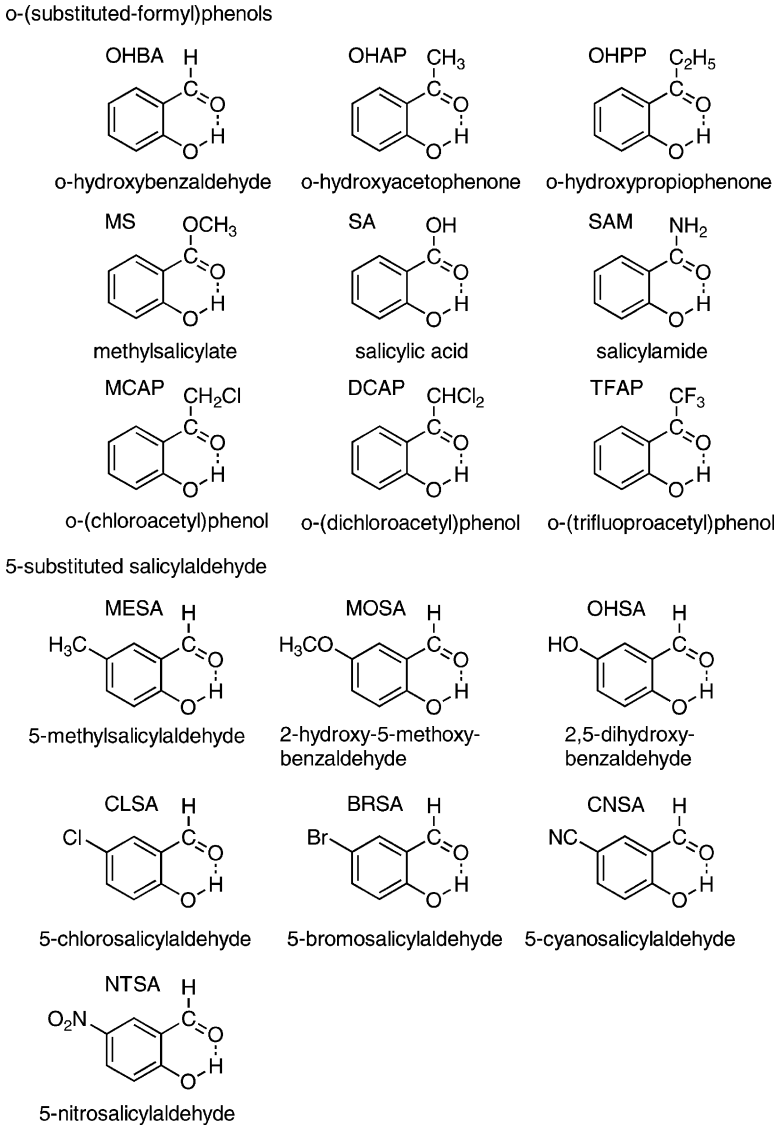

Fig. 1. Structures of the molecules studied in the present work.

In this paper, we apply our nodal-plane model to the substituent effect in the ESIPT of OHBAs. The structures of the molecules studied in this work are shown in Fig. 1. The next section briefly summarizes the mechanism of ESIPT according to our nodal-plane model. The following section describes our experiments with OHBAs and shows that the results of those experiments are consistent with our nodal-plane model. The last section summarizes our conclusions.

2. Nodal-plane model of ESIPT

OHBA can exist in two tautomeric forms: the keto form and the enol form (proton-transferred form). The relative stability of each form depends on the electronic state of the molecule, as shown in Fig. 2: in the ground state (S_0 state) the keto form is stable, in the first excited $^1(\pi, \pi^*)$ state ($S_1^{(\pi)}$ state) ESIPT takes place and yields the enol form, and in the second excited $^1(\pi, \pi^*)$ state ($S_2^{(\pi)}$ state) the keto form is again stable [15,17].

The equilibrium constant between the enol forms of acetylacetaldehyde [$CH_3C(OH)$=CHCHO (A form) and CH_3COCH=CHOH (B form)] has been determined by NMR [60]. The broken curve in Fig. 3 (double-minimum potential) shows the potential curves of the two forms. The enol forms of malonaldehyde [HC(OH)=CHCHO] can also be characterized by a double-minimum potential [61–66]. Substituting phenyl rings for the CH_3CCH moieties in the acetylacetaldehyde enols respectively transforms the A and B forms into the keto and enol forms of OHBA (Fig. 3). The substitution stabilizes the A form due to the resonance of the phenyl ring [67], and the keto form of OHBA becomes markedly lower in energy than the A form of acetylacetaldehyde. The B form, in contrast, is not stabilized by the

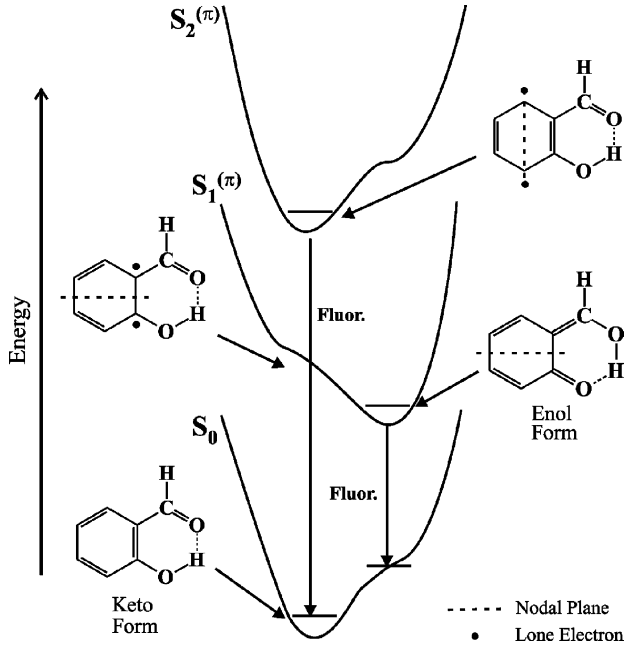

Fig. 2. Schematic representation of the S_0, $S_1^{(\pi)}$ and $S_2^{(\pi)}$ potential surfaces for OHBA. Fluor. denotes fluorescence. The broken lines indicate the nodal planes perpendicular to the molecular plane, and the dots indicate seemingly lone π electrons.

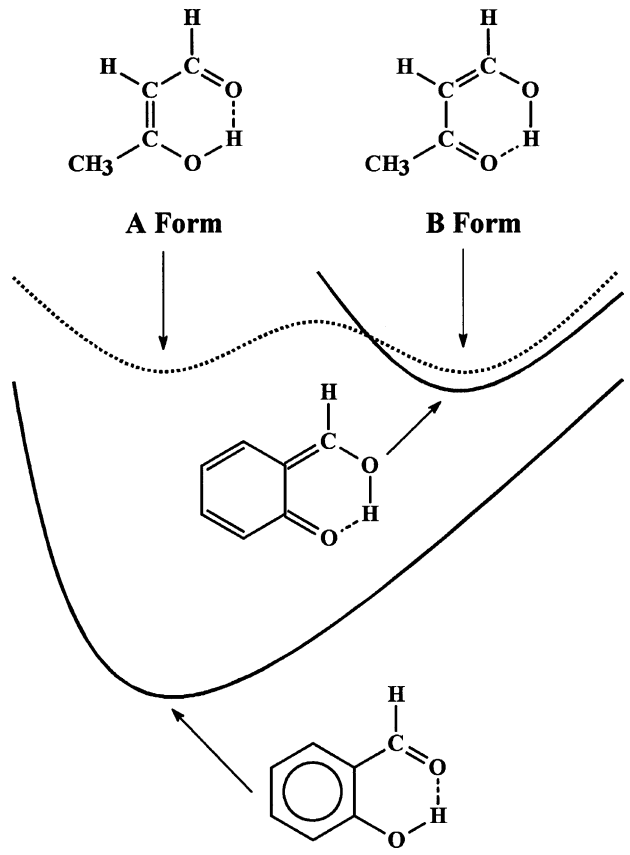

Fig. 3. Potential curves of acetylacetaldehyde enols (broken curve) [60] and OHBA (continuous curves).

substitution, and its energy remains essentially unchanged in transforming to the enol form of OHBA. The schematic sketch of the potential curves of OHBA thus obtained (the continuous curves in Fig. 3) is quite similar to that expected from experimental results [13,14] for the S_0 and $S_1^{(\pi)}$ states of OHBA (Fig. 2): the $S_1^{(\pi)}$ state is thought to be much more susceptible to ESIPT than the S_0 state. Based on Fig. 3, we suggest that the presence of the phenyl ring has a large influence on the potential curves of the S_0 and $S_1^{(\pi)}$ states of OHBA.

Fig. 4 shows the nodal planes of the wave functions in several states of benzene and OHBA. As in the case of a particle in a two-dimensional rectangular potential box [68], the wave function of the S_0 state has no nodal plane, while the wave functions of the S_1 and S_2 states each have one nodal plane, and these nodal planes are perpendicular to each other. In the usual notation, the S_1 and S_2 states of benzene [$^1(\pi, \pi^*)$ states] are designated as L_b and L_a, respectively [69]. Substituting CHO and OH groups for adjacent H atoms in benzene produces OHBA (Fig. 4).

In the L_a state, one can write two double bonds along the nodal plane, because π electrons are distributed over the molecule except on the nodal plane. When the two double bonds are C_3=C_4 and C_5=C_6, lone π electrons are localized at the C_1 and C_2 atoms (Fig. 4). If ESIPT yielding the enol form takes place in the L_a state of OHBA, the two lone electrons can be largely delocalized due to the formation of the C_1=C_0 and C_2=O_2 bonds. The lone electrons thus facilitate the rearrangement of the bonds to produce the enol form. The L_a state of the enol form of OHBA thus becomes significantly lower in energy than the L_a state of benzene

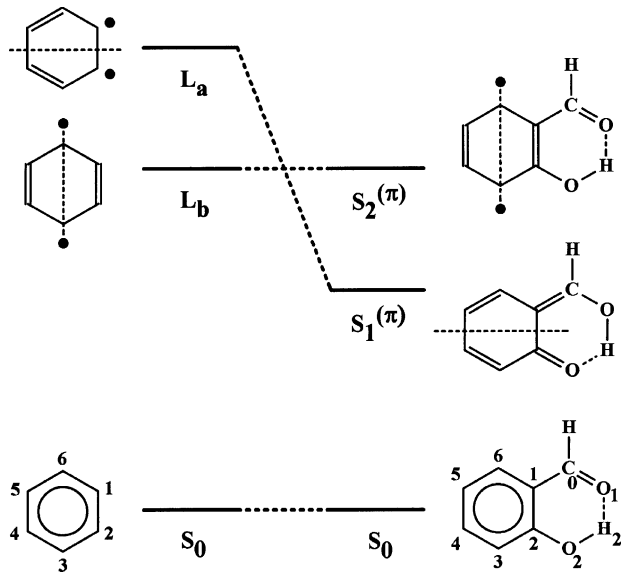

Fig. 4. Nodal planes of the wave functions in several $^1(\pi, \pi^*)$ states of benzene and OHBA and the numbering system for the atoms. The broken lines indicate nodal planes perpendicular to the molecular plane, and the dots indicate seemingly lone π electrons. Only one of the three positions of the nodal plane for the excited state of benzene is shown.

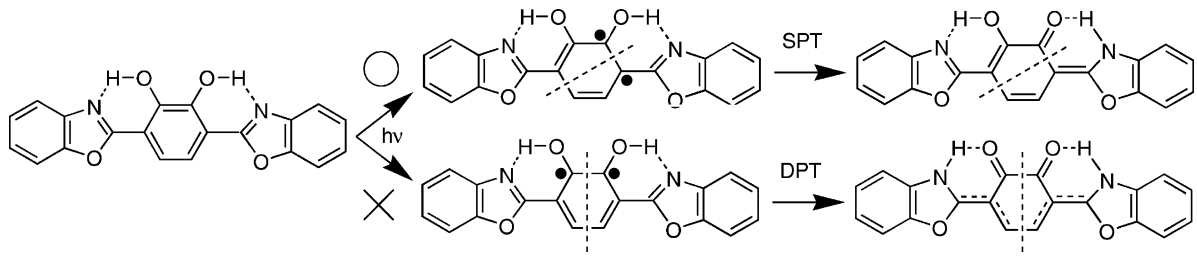

Scheme 1.

due to the delocalization, and in OHBA the L_a state results in the $S_1^{(\pi)}$ state (Fig. 4). The enol form is preferred because of the more favorable nodal pattern in the $S_1^{(\pi)}$ state of OHBA.

In contrast, the wave function in the L_b state of OHBA has a nodal plane perpendicular to that in the L_a state (Fig. 4). ESIPT yielding the enol form cannot take place in the L_b state because $C_0{=}C_1$ and $C_2{=}O_2$ double bonds cannot be formed: if these double bonds were formed, the C_1 and C_2 atoms would become pentavalent. As a result, the potential energy of the L_b state remains essentially unchanged in transforming from benzene to OHBA, and the potential curve is not distorted much from that of the S_0 state of OHBA. In OHBA, the L_b state thus results in the $S_2^{(\pi)}$ state (Fig. 4).

For these reasons the $S_2^{(\pi)}$ state of OHBA is thought to be far less susceptible to ESIPT than the $S_1^{(\pi)}$ state. This hypothesis is consistent with the emission properties of OHBAs [13–21,25,27,28]. We are therefore led to the conclusion that the enol form is stabilized in the $S_1^{(\pi)}$ state due to the properties of the nodal plane of the wave function. In terms of our nodal-plane model, ESIPT is described as a skeletal distortion of the aromatic ring instead of as a change in the O–H···O structure. The structural reorganization in ESIPT is not localized around the hydrogen bond, but rather encompasses the molecular framework. Therefore, in terms of our nodal-plane model, what we refer to as ESIPT is more accurately described as "hydrogen transfer," "keto–enol tautomerization" or "hydrogen translocation." For consistency with previous usage, however, in this paper we use the designation "proton transfer."

In our view, whether ESIPT occurs easily in an intramolecularly hydrogen-bonded molecule can be predicted directly from the wave function itself: the aromatic skeleton responds to the formation of the node in the $S_1^{(\pi)}$ wave function. Our concept is simple and readily provides a qualitative guide useful for predicting the most stable form in a particular electronic state. We can predict the stabilization due to ESIPT of medium-size polyatomic molecules without performing extensive calculations.

We should note that if for some reason the excited $^1(n, \pi^*)$ state ($S_1^{(n)}$ state) is located much below the $S_1^{(\pi)}$ state, the simple generalization of our model to ESIPT of such a molecule does not make sense. Douhal et al. [9] noted that our nodal-plane picture cannot explain the absence of ESIPT in 3-(2-hydroxyphenyl)imidazo[1,5-*a*]pyridine (HPIP). However, the reason for the inconsistency between the absence of ESIPT in HPIP and our model is quite simple. As Douhal et al. [70] themselves noted, the S_1 state is assigned to (n,π^*) in HPIP and located much below the $S_1^{(\pi)}$ state. Formal comparison between the absence of ESIPT in HPIP and our model is thus not appropriate. In view of the electronic structure of a state of the (n,π^*) type, it is hardly conceivable that "proton" transfer and hydrogen-bond formation occur in the $S_1^{(n)}$ state, as already pointed out by Nagaoka et al. [15].

It should also be noted that our model may not be able to predict real situations when the $S_1^{(\pi)}$ state is represented by extensive mixture of various configurations. Our preliminary calculated results for the lowest excited triplet state of [2,2′-bipyridine]-3,3′-diol support this view [71]. As another example, we should mention ESIPT in 3,6-bis(benzoxazolyl)pyrocatechol (BBPC). BBPC was assigned and reported by Grabowska et al. [37] as an example of an excited-state double-proton-transfer (DPT) reaction producing a diketo-tautomer. The nodal-plane model confirmed the DPT mechanism in BBPC by taking into account the delocalization of the double bonds (Scheme 1) [27,30]. Such delocalization derives from the situation that the $S_1^{(\pi)}$ state is represented by extensive mixture of various configurations. However, only recently Grabowska and co-workers [51] had to revise the DPT mechanism and concluded that BBPC undergoes a single-proton-transfer (SPT) in the $S_1^{(\pi)}$ state. In fact, our recent calculation, as well as that by Zgierski et al. [72], showed that the $S_1^{(\pi)}$ wave function of BBPC is dominated by the one-electron-excitation configuration rather than being represented by extensive mixture of various configurations. Accordingly, it is reasonable to assume that the extensive delocalization of the double bonds would be absent here, and that BBPC undergoes SPT in the $S_1^{(\pi)}$ state. However, as shown in Scheme 1, the SPT reaction scheme of BBPC can nonetheless be explained in terms of our nodal-plane model.

3. Substituent effect in ESIPT of OHBAs

In this section, we examine the absorption and fluorescence spectra of various OHBAs and discuss how

these experimental results strongly support our nodal-plane model.

3.1. Experimental methods

Sample preparation. *o*-(Trifluoroacetyl)phenol (TFAP) [73,74], *o*-(chloroacetyl)phenol (MCAP) [75–77], *o*-(dichloroacetyl)phenol (DCAP) [75–77], 5-methylsalicylaldehyde (MESA) [78–80] and 5-cyanosalicylaldehyde (CNSA) [78–80] were synthesized according to the methods reported previously. TFAP, DCAP and CNSA were purified by column chromatography. MCAP and MESA were recrystallized twice from petroleum ether and chloroform, respectively. OHBA, MS, SA, *o*-hydroxyacetophenone (OHAP), *o*-hydroxypropiophenone (OHPP), salicylamide (SAM), 2-hydroxy-5-methoxybenzaldehyde (MOSA), 5-chlorosalicylaldehyde (CLSA), 5-bromosalicylaldehyde (BRSA), 5-nitrosalicylaldehyde (NTSA) and 2,5-dihydroxybenzaldehyde (OHSA) were commercially obtained. OHBA, MS, OHAP, OHPP and MOSA were purified by distillation under reduced pressure. SA and SAM were recrystallized twice from chloroform. CLSA and BRSA were recrystallized twice from petroleum ether. NTSA and OHSA were recrystallized twice from a mixed solvent of petroleum ether and chloroform. Hexane and cyclohexane, which were used for spectral measurements of the *o*-(substituted-formyl)phenols (TFAP, MCAP, DCAP, OHBA, MS, SA, OHAP, OHPP and SAM) and 5-substituted salicylaldehydes (MESA, CNSA, MOSA, CLSA, BRSA, NTSA and OHSA), respectively, were specially prepared for luminescence and used without further purification.

Measurements. Experiments were conducted at room temperature with a 1 cm^2 quartz cell. The sample concentrations were about 10^{-5}–10^{-4} M. Before measuring at room temperature, the sample solutions were degassed by bubbling argon gas through them. The absorption spectra were measured with a Shimadzu UV-2100S spectrophotometer, while the fluorescence spectra were measured with a Shimadzu RF-5000 spectrofluorophotometer. The fluorescence spectrum signals were transferred to a microcomputer and analyzed by using the method of Mimuro et al. [81]. The fluorescence quantum yields (ϕ_f's) were determined by comparing the fluorescence spectra of the samples with that of quinine sulfate in 1 N sulfuric acid [82], after the fluorescence spectra concerned had been corrected for the spectral sensitivity of the detector. Although MS and SA show dual fluorescence [83], from the fluorescence spectra we only derived the long-wavelength emission originating from proton-transferred species by using the method of Mimuro et al. [81] and determined the ϕ_f's.

3.2. Factors influencing ϕ_f

In the decay from the $S_1^{(\pi)}$ states of OHBAs, the nonradiative decay rate constant (k_{nr}) is much larger than the radiative one (k_r), as seen from the small ϕ_f of OHBA [13]. Candidates for the nonradiative decay process from the $S_1^{(\pi)}$ state include $S_1^{(\pi)} \rightarrow S_0$ internal conversion and intersystem crossing to a triplet state. The $S_1^{(\pi)} \rightarrow S_0$ decay rate constant in a solution can be analyzed in terms of the sum of the temperature-independent and -dependent decay rate constants [13,14,84]. The intersystem crossing and the radiative process in the enol tautomer are temperature-independent, while the temperature-dependent decay process, which is dominant at room temperature, has been identified as the $S_1^{(\pi)} \rightarrow S_0$ internal conversion [85]. Accordingly, it seems likely that the $S_1^{(\pi)} \rightarrow S_0$ internal conversion would be dominant in the nonradiative decay from the $S_1^{(\pi)}$ state under the present experimental conditions.

ϕ_f can be expressed with the following equation:

$$\phi_f = \frac{k_r}{k_{nr} + k_r}. \tag{1}$$

Since k_r is very small (as described above), $k_{nr} + k_r$ is almost equal to k_{nr}. Thus, ϕ_f can be written as follows:

$$\phi_f = \frac{k_r}{k_{nr}}. \tag{2}$$

ϕ_f is proportional to the reciprocal of the $S_1^{(\pi)} \rightarrow S_0$ internal-conversion rate (k_{nr}), where k_{nr} is proportional to exp $(-\Delta E_{10}^a)$ according to the energy-gap law [86] and ΔE_{10}^a denotes the energy difference between the zero-point vibrational levels of the $S_1^{(\pi)}$ and S_0 states; that is, the adiabatic transition energy between them. Thus,

$$\log \phi_f \propto -\log k_{nr} \propto \Delta E_{10}^a. \tag{3}$$

3.3. Results and discussion

o-(Substituted-formyl)phenols. Fig. 5a shows an example of absorption and fluorescence spectra of *o*-(substituted-formyl)phenols. The ϕ_f's of the *o*-(substituted-formyl)phenols are given in Table 1, together with Yukawa and Tsuno's σ_π constants [87–89] for the substituents bonded to the carbonyl carbon. The value of ϕ_f decreases with increasing σ_π. σ_π is a type of Hammett parameter. The Hammett equation is given by

$$\log x(n) = \rho \cdot \sigma(n) + \text{const}, \tag{4}$$

Table 1
Yukawa and Tsuno's σ_π constants [87–89] for various substituents, and ϕ_f and ΔE_{abs} for *o*-(substituted-formyl)phenols in hexane

Molecule	Substituent	σ_π Constant	ϕ_f	ΔE_{abs} (eV)
TFAP	CF_3	+0.24	1.6×10^{-5}	3.562
DCAP	$CHCl_2$		5.2×10^{-5}	3.586
MCAP	CH_2Cl		9.7×10^{-5}	3.689
OHBA	H	±0	8.6×10^{-4}	3.793
OHAP	CH_3	−0.078	1.1×10^{-3}	3.818
OHPP	C_2H_5	−0.069	8.4×10^{-4}	3.833
MS	OCH_3	−0.281	1.4×10^{-2}	4.032
SA	OH	−0.34	1.6×10^{-2}	3.985
SAM	NH_2	−0.42	3.4×10^{-2}	4.024

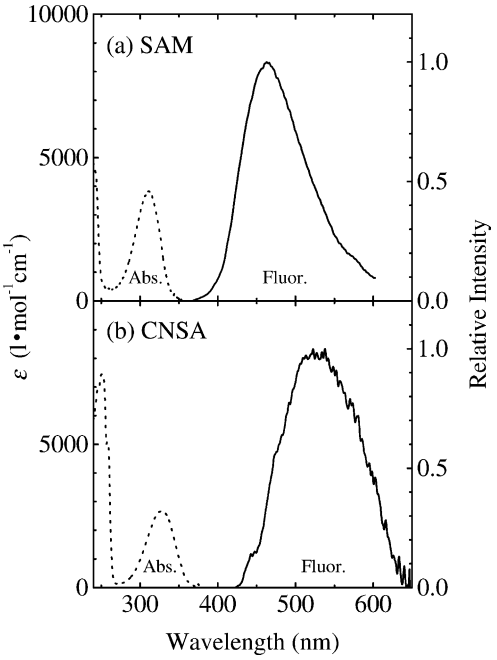

Fig. 5. Absorption (Abs.) and fluorescence (Fluor.) spectra of (a) SAM in hexane and (b) CNSA in cyclohexane. ε denotes the absorption coefficient. The fluorescence spectra have been corrected for the spectral sensitivity of the detector. The fluorescence spectra of SAM and CNSA were obtained by excitation at 311.0 and 333.6 nm, respectively.

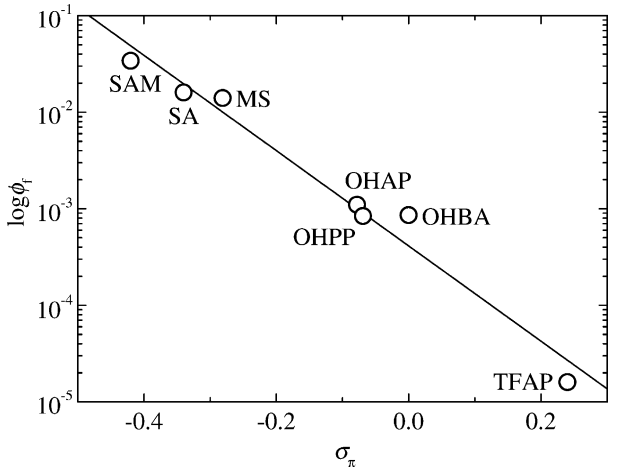

Fig. 6. Plot of $\log \phi_f$ against σ_π for *o*-(substituted-formyl)phenols. The plot gives a good linear fit with a slope of −4.93, an intercept of 4.13×10^{-4} and a correlation coefficient of 0.986.

where $x(n)$ denotes an experimental value for a molecule with substituent n, ρ a characteristic parameter for a given reaction, and $\sigma(n)$ a characteristic parameter for substituent n. Yukawa and Tsuno expressed a parameter corresponding to σ in the Hammett equation as $\sigma_i + r\sigma_\pi$, where σ_i is a normal substituent constant that does not involve any additional π-electronic interaction between a substituent and the reaction center. σ_π is the resonance substituent constant, measuring the capability for π-delocalization of a π-electron-donating or π-electron-withdrawing substituent. As the electron-withdrawing property of a substituent bonded to the carbonyl carbon becomes stronger, σ_π increases. r is a characteristic parameter for a given reaction and measures the extent of resonance demand. The value of σ_π does not depend on the substituted position. The reference system used in developing these parameters was the same as that used for the Hammett equation. Yukawa and Tsuno's constants are applicable to various substituted positions of many molecules [87–89]. Since the change in electronic structure due to the $S_0 \rightarrow S_1^{(\pi)}$ excitation [(π,π^*) transition] mainly affects the π-bonding framework of the aromatic ring moiety, as mentioned in Section 2, the σ_π constant is the most suitable choice as the Hammett parameter for analyzing the present experimental results. We thus plotted $\log \phi_f$ against the σ_π value (Fig. 6). The plot shows a good linear relationship with a negative slope, so that as σ_π increases, ϕ_f decreases.

This substituent effect can be explained by considering the nodal pattern of the wave function and the delocalization of the lone electrons in the excited states (Fig. 7). In a molecule with an electron-withdrawing substituent at the formyl group, the lone π electron on C_1 is significantly delocalized in the $S_1^{(\pi)}$ state (the curved arrow in Fig. 7). Due to the delocalization of the lone electron on C_1, the $S_1^{(\pi)}$ state is stabilized in comparison with that of OHBA. Then, ΔE_{10}^a decreases (Fig. 7), and as a result, the $S_1^{(\pi)} \rightarrow S_0$ internal-conversion rate constant (k_{nr}) increases (Eq. (3)) according to the energy-gap law [86]. Since ϕ_f decreases as k_{nr} increases (Eqs. (1)–(3)), the ϕ_f value must be less than that of OHBA. The situation for a molecule with an electron-donating substituent at the formyl group is the reverse of that with an electron-withdrawing substituent. The substituent effects observed here support our nodal-plane model.

If the $S_1^{(\pi)}$ potential surfaces of *o*-(substituted-formyl)-phenols are similar in shape to one another and only ΔE_{10}^a is changed by the substituent effect, the vertical $S_0 \rightarrow S_1^{(\pi)}$ transition energy (ΔE_{10}^v) decreases and the photon energy at the $S_0 \rightarrow S_1^{(\pi)}$ absorption maximum (ΔE_{abs}) decreases with decreasing ΔE_{10}^a (Fig. 7). Then, ΔE_{abs} is expected to decrease with increasing σ_π according to our nodal-plane model. The values of ΔE_{abs} are listed in Table 1. As the electron-withdrawing property of the substituent bonded to the carbonyl carbon becomes stronger (that is, as σ_π increases), ΔE_{abs} decreases. These results are also consistent with our model.

If these substituent effects based on our nodal-plane model were absent, ϕ_f would not show systematic dependence on the electron-donating and electron-withdrawing properties of the substituent. In fact, the $S_1 \rightarrow S_0$ fluorescence quantum yields of benzene, 1,4-bis-(trifluoromethyl)benzene (CF_3–Ph–CF_3), *p*-xylene (CH_3–Ph–CH_3) and 1,4-dimethoxybenzene (CH_3O–Ph–OCH_3) in cyclohexane were estimated to be 0.07, 0.16, 0.40 and 0.21, respectively [90]. These values do not show a systematic substituent effect,

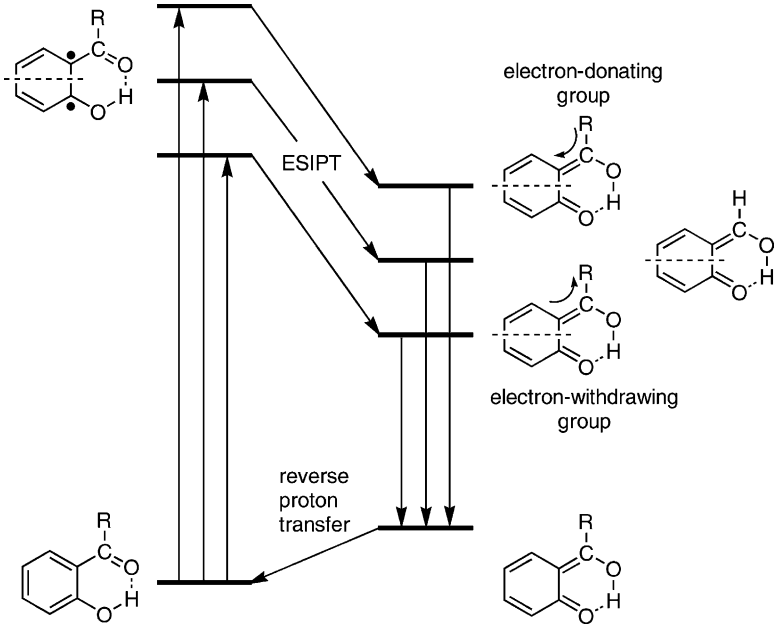

Fig. 7. Schematic energy-state diagram for dynamic processes in the $S_1^{(\pi)}$ and S_0 states of *o*-(substituted-formyl)phenols. The substituent effect on the ground-state energy of the proton-transferred species is not included in this figure.

in contrast to the ϕ_f's of OHBA, TFAP, OHAP and MS in Table 1.

5-Substituted salicylaldehydes. Fig. 5b shows an example of absorption and fluorescence spectra of 5-substituted salicylaldehydes. The ϕ_f's of the 5-substituted salicylaldehydes are given in Table 2, together with Yukawa and Tsuno's σ_π constants [87–89] for the substituents at the 5-position. As with the *o*-(substituted-formyl)phenols, the value of ϕ_f decreases with increasing σ_π, and a plot of $\log\phi_f$ against the σ_π value (Fig. 8) indicates a fair linear relationship with a negative slope. As the electron-withdrawing property of the substituent at the 5-position becomes stronger, ϕ_f decreases.

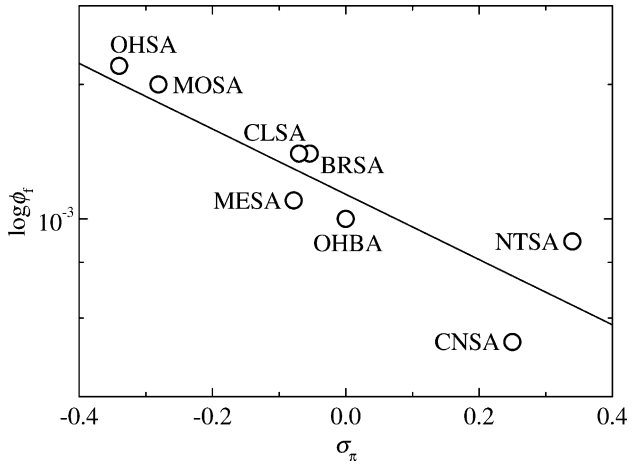

Fig. 8. Plot of $\log\phi_f$ against σ_π for 5-substituted salicylaldehydes. The plot gives a fair linear fit with a slope of −0.731, an intercept of 1.14×10^{-3} and a correlation coefficient of 0.848.

This substituent effect can also be explained by considering the nodal pattern of the wave function and the delocalization of the lone electrons in the excited states (Fig. 9). In a molecule with an electron-withdrawing substituent at the 5-position, the lone π electron on C_1 is delocalized in the $S_1^{(\pi)}$ state (the wavy arrow in Fig. 9). Due to the delocalization, ΔE_{10}^a decreases, k_{nr} increases and ϕ_f decreases (Eq. (3)), just as for *o*-(substituted-formyl)phenols.

The absolute value of the slope of the plot in Fig. 8 is much less than that in Fig. 6. Thus, the effect of a substituent at the 5-position on ϕ_f is much less than that of a substituent bonded to the carbonyl carbon. This can be attributed to the fact that the distance between the substituent and the C_1 atom is longer in 5-substituted salicylaldehydes than in *o*-(substituted-formyl)phenols.

The values of ΔE_{abs} for the 5-substituted salicylaldehydes are listed in Table 2. ΔE_{abs} *increases* (that is, ΔE_{10}^v increases) as the electron-withdrawing property of the substituent at the 5-position becomes stronger (that is, as σ_π

Table 2
Yukawa and Tsuno's σ_π constants [87–89] for various substituents, and ϕ_f and ΔE_{abs} for 5-substituted salicylaldehydes in cyclohexane

Molecule	Substituent	σ_π Constant	ϕ_f	ΔE_{abs} (eV)
NTSA	NO_2	+0.34	8.9×10^{-4}	3.779
CNSA	CN	+0.25	5.3×10^{-4}	3.788
OHBA	H	±0	1.0×10^{-3}	3.784
BRSA	Br	−0.054	1.4×10^{-3}	3.626
CLSA	Cl	−0.070	1.4×10^{-3}	3.629
MESA	CH_3	−0.078	1.1×10^{-3}	3.656
MOSA	OCH_3	−0.281	2.0×10^{-3}	3.426
OHSA	OH	−0.34	2.2×10^{-3}	3.422

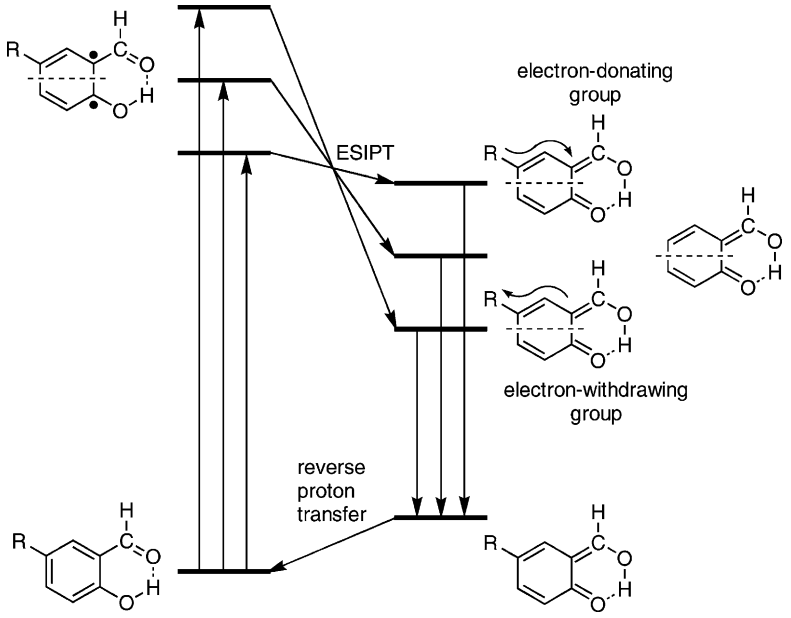

Fig. 9. Schematic energy-state diagram for dynamic processes in the $S_1^{(\pi)}$ and S_0 states of 5-substituted salicylaldehydes. The substituent effect on the ground-state energy of the proton-transferred species is not included in this figure.

increases). However, this result contrasts with the results for *o*-(substituted-formyl)phenols (Table 1), which show that ΔE_{abs} *decreases* (that is, ΔE_{10}^{v} decreases) as the electron-withdrawing property of the substituent becomes stronger (that is, as σ_π increases). The fact that ΔE_{10}^{a} decreases and ΔE_{10}^{v} increases as the electron-withdrawing property of the substituent at the 5-position becomes stronger shows that the shape of the $S_1^{(\pi)}$ potential surface of 5-substituted salicylaldehydes is changed by the substituent effect, in contrast to the case of *o*-(substituted-formyl)-phenols. That is, as the electron-withdrawing property of the substituent at the 5-position becomes stronger, the potential is stabilized according to our nodal-plane model, but the curvature of the potential increases (Fig. 9). As a result, ΔE_{10}^{a} decreases but ΔE_{10}^{v} increases. In 5-substituted salicylaldehydes, the nodal property is not the only factor influencing the spectral property, because the nodal effect of the substituent at the 5-position on the $S_1^{(\pi)}$ potential surface is, as noted above, much less than that at the formyl group in *o*-(substituted-formyl)phenols.

Another candidate factor influencing the spectral property of 5-substituted salicylaldehydes is as follows. In the L_a state of 5-substituted salicylaldehydes, a positive charge is preferred for the substituent at the 5-position, because a lone π electron is localized on the C_1 atom and positive and negative charges tend to alternate on the molecular frame (Scheme 2a). When the substituent has an electron-withdrawing property, this charge distribution makes the L_a state unstable and increases ΔE_{10}^{v}. On the other hand, when the substituent has an electron-donating property, the charge distribution stabilizes the L_a state and decreases ΔE_{10}^{v}. The situation for *o*-(substituted-formyl)phenols

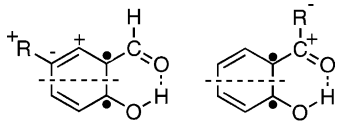

Scheme 2.

is the reverse of that for 5-substituted salicylaldehydes because a negative charge is preferred for the substituent bonded to the carbonyl carbon (Scheme 2b). As a result, with respect to the spectral property of *o*-(substituted-formyl)-phenols, the influence of this factor is opposite to that expected for 5-substituted salicylaldehydes. This concept is also consistent with the experimental results (Figs. 7 and 9).

4. Conclusions

The ESIPT of OHBAs in solution has been studied by emission spectroscopy. Substituent effects on ϕ_f can be explained by considering the nodal pattern of the wave function along with the delocalization of the π electrons in the excited state. The substituent effect in 5-substituted salicylaldehydes is much less than that in *o*-(substituted-formyl)phenols.

Acknowledgements

We are indebted to Dr. Keishi Ohara of Ehime University for his experimental support. SN also thanks Professor Emeritus Noboru Hirota of Kyoto University and Professor Kazuo Mukai of Ehime University for their continuous

encouragement. Last but not least, SN expresses his sincere thanks to Professor Ronald P. Steer of the University of Saskatchewan for his kind invitation to submit a paper for publication in this special issue of the Journal of Photochemistry and Photobiology, A: Chemistry, devoted to "Photon-Initiated Proton Transfer."

References

[1] W. Klöffer, Adv. Photochem. 10 (1977) 311.
[2] P.M. Rentzepis, P.F. Barbara, Adv. Chem. Phys. 47 (2) (1981) 627.
[3] D. Huppert, M. Gutman, K.J. Kaufmann, Adv. Chem. Phys. 47 (2) (1981) 643.
[4] M. Kasha, J. Chem. Soc., Faraday Trans. II 82 (1986) 2379 (Review).
[5] P.F. Barbara, P.K. Walsh, L.E. Brus, J. Phys. Chem. 93 (1989) 29 (Feature Article).
[6] P.F. Barbara, H.P. Trommsdorff, R.M. Hochstrasser, G.L. Hofacker (Eds.), Spectroscopy and Dynamics of Elementary Proton Transfer in Polyatomic Systems, Chem. Phys. 136 (1989) 153–360.
[7] P.F. Barbara, M. Nicol, M.A. El-Sayed (Eds.), M. Kasha Festschrift J. Phys. Chem. 95 (1991) 10215–10524.
[8] S.J. Formosinho, L.G. Arnaut, J. Photochem. Photobiol. A 75 (1993) 21 (Review).
[9] A. Douhal, F. Lahmani, A.H. Zewail, Chem. Phys. 207 (1996) 477 (Review).
[10] T. Sugawara, I. Takasu, Adv. Phys. Org. Chem. 32 (1999) 219.
[11] S. Scheiner, J. Phys. Chem. A 104 (2000) 5898 (Feature Article).
[12] S. Nagaoka, A. Nakamura, U. Nagashima, J. Phys. Chem. 154 (2002) 23.
[13] S. Nagaoka, N. Hirota, M. Sumitani, K. Yoshihara, J. Am. Chem. Soc. 105 (1983) 4220.
[14] S. Nagaoka, N. Hirota, M. Sumitani, K. Yoshihara, E. Lipczynska-Kochany, H. Iwamura, J. Am. Chem. Soc. 106 (1984) 6913.
[15] S. Nagaoka, M. Fujita, T. Takemura, H. Baba, Chem. Phys. Lett. 123 (1986) 489.
[16] S. Nagaoka, J. Photochem. Photobiol. A 40 (1987) 185.
[17] S. Nagaoka, U. Nagashima, N. Ohta, M. Fujita, T. Takemura, J. Phys. Chem. 92 (1988) 166.
[18] S. Nagaoka, U. Nagashima, Chem. Phys. 136 (1989) 153.
[19] S. Nagaoka, Chem. Chem. Ind. 44 (1991) 182.
[20] U. Nagashima, S. Nagaoka, S. Katsumata, J. Phys. Chem. 95 (1991) 3532.
[21] E. Hoshimoto, S. Yamauchi, N. Hirota, S. Nagaoka, J. Phys. Chem. 95 (1991) 10229.
[22] S. Nagaoka, A. Itoh, K. Mukai, E. Hoshimoto, N. Hirota, Chem. Phys. Lett. 192 (1992) 532.
[23] S. Nagaoka, A. Itoh, K. Mukai, U. Nagashima, J. Phys. Chem. 97 (1993) 11385.
[24] S. Nagaoka, U. Nagashima, Chem. Phys. 206 (1996) 353.
[25] S. Nagaoka, Y. Shinde, K. Mukai, U. Nagashima, J. Phys. Chem. A 101 (1997) 3061.
[26] S. Nagaoka, S. Yamamoto, K. Mukai, J. Photochem. Photobiol. A 105 (1997) 29.
[27] S. Nagaoka, U. Nagashima, Trends Phys. Chem. 6 (1997) 55.
[28] S. Nagaoka, U. Nagashima, Photochemistry 28 (1998) 39.
[29] S. Nagaoka, J. Kusunoki, T. Fujibuchi, S. Hatakenaka, K. Mukai, U. Nagashima, J. Photochem. Photobiol. A 122 (1999) 151.
[30] S. Nagaoka, U. Nagashima, J. Phys. Chem. 94 (1990) 1425.
[31] S. Nagaoka, U. Nagashima, J. Phys. Chem. 95 (1991) 4006.
[32] P.-T. Chou, J. Chinese Chem. Soc. 48 (2001) 651.
[33] A. Grabowska, A. Mordziński, N. Tamai, K. Yoshihara, Chem. Phys. Lett. 153 (1988) 389.
[34] S.L. Studer, P.-T. Chou, D. McMorrow, Chem. Phys. Lett. 161 (1989) 361.
[35] P.-T. Chou, M.L. Martinez, S.L. Studer, J. Phys. Chem. 94 (1990) 3639.
[36] A. Grabowska, A. Mordziński, N. Tamai, K. Yoshihara, Chem. Phys. Lett. 169 (1990) 450.
[37] A. Grabowska, A. Mordziński, K. Kownacki, E. Gilabert, C. Rullière, Chem. Phys. Lett. 177 (1991) 17.
[38] A. Held, D.F. Plusquellic, J.L. Tomer, D.W. Pratt, J. Phys. Chem. 95 (1991) 2877.
[39] A. Grabowska, J. Sepioł, C. Rullière, J. Phys. Chem. 95 (1991) 10493.
[40] J.L. Herek, S. Pedersen, L. Bañares, A.H. Zewail, J. Chem. Phys. 97 (1992) 9046.
[41] A.L. Sobolewski, W. Domcke, Chem. Phys. 184 (1994) 115.
[42] K.-Y. Law, J. Shoham, J. Phys. Chem. 98 (1994) 3114.
[43] M.V. Vener, S. Scheiner, J. Phys. Chem. 99 (1995) 642.
[44] A. Jaworski, A. Degórski, Comp. Chem. 19 (1995) 189.
[45] P.B. Bisht, H. Petek, K. Yoshihara, U. Nagashima, J. Chem. Phys. 103 (1995) 5290.
[46] A.L. Sobolewski, W. Domcke, in: D. Heidrich (Ed.), The Reaction Path in Chemistry: Current Approaches and Perspectives, Kluwer Academic Publishers, Amsterdam, 1995, pp. 257–282.
[47] T. Sekikawa, T. Kobayashi, T. Inabe, J. Phys. Chem. B 101 (1997) 10645.
[48] M.P. Marzocchi, A.R. Mantini, M. Casu, G. Smulevich, J. Chem. Phys. 108 (1998) 534.
[49] A.L. Sobolewski, W. Domcke, Chem. Phys. 232 (1998) 257.
[50] S. Tobita, M. Yamamoto, N. Kurahayashi, R. Tsukagoshi, Y. Nakamura, H. Shizuka, J. Phys. Chem. A 102 (1998) 5206.
[51] R. Wortmann, S. Lebus, H. Reis, A. Grabowska, K. Kownacki, S. Jarosz, Chem. Phys. 243 (1999) 295.
[52] S. Mitra, N. Tamai, Chem. Phys. 246 (1999) 463.
[53] A.O. Doroshenko, E.A. Posokhov, A.A. Verezubova, L.M. Ptyagina, J. Phys. Org. Chem. 13 (2000) 253.
[54] S. Takeuchi, T. Tahara, J. Phys. Chem. A 102 (1998) 7740.
[55] P.-T. Chou, G.-R. Wu, C.-Y. Wei, C.-C. Cheng, C.-P. Chang, F.-T. Hung, J. Phys. Chem. B 104 (2000) 7818.
[56] D.M. Friedrich, Z. Wang, A.G. Joly, K.A. Peterson, P.R. Callis, J. Phys. Chem. A 103 (1999) 9644.
[57] W. Eberbach, J. Hensle, Tetrahedr. Lett. 34 (1993) 4773.
[58] W. Eberbach, J. Hensle, Tetrahedr. Lett. 34 (1993) 4777.
[59] K. Sakai, G. Vacek, H.P. Lüthi, U. Nagashima, Photochem. Photobiol. 66 (1997) 532.
[60] J. Castells, J. Soler, An. Quim. 72 (1976) 1037;
J. Castells, J. Soler, Chem. Abstr. 87 (25) (1977) 200661z.
[61] W.F. Rowe, R.W. Duerst, E.B. Wilson, J. Am. Chem. Soc. 98 (1976) 4021.
[62] P. Turner, S.L. Baughcum, S.L. Coy, Z. Smith, J. Am. Chem. Soc. 106 (1984) 2265.
[63] D.W. Firth, P.F. Barbara, H.P. Trommsdorff, Chem. Phys. 136 (1989) 349, and references cited therein.
[64] N. Shida, P.F. Barbara, J.E. Almlöf, J. Chem. Phys. 91 (1989) 4061.
[65] T. Chiavassa, P. Roubin, L. Pizzala, P. Verlaque, A. Allouche, F. Marinelli, J. Phys. Chem. 96 (1992) 10659, and references cited therein.
[66] T.D. Sewell, Y. Guo, D.L. Thompson, J. Chem. Phys. 103 (1995) 8557, and references cited therein.
[67] G. Herzberg, Molecular Spectra and Molecular Structure III. Electronic Spectra and Electronic Structure of Polyatomic Molecules, Van Nostrand Reinhold, New York, 1966, Chapter III.
[68] P.W. Atkins, J. de Paula, Atkins' Physical Chemistry, 7th ed., Oxford University Press, Oxford, 2002, pp. 331–334.
[69] J.B. Birks (Ed.), Organic Molecular Photophysics, vol. 1, Wiley, London, 1973, Chapter 1.
[70] A. Douhal, F. Amat-Guerri, A.U. Acuña, J. Phys. Chem. 99 (1995) 76.
[71] S. Nagaoka, U. Nagashima, Abstracts of 1992 Symposium on Molecular Science, Kyoto, 1A19.

[72] M.Z. Zgierski, A. Fernández-Ramos, A. Grabowska, J. Chem. Phys. 116 (2002) 7486.
[73] L. Benoiton, H.N. Rydon, J.E. Willett, Chem. Ind. (London) (1960) 1060.
[74] S. Matsumoto, H. Kobayashi, K. Ueno, Bull. Chem. Soc. Jpn. 42 (1969) 960.
[75] H.H. Bosshard, R. Mory, M. Schmid, H. Zollinger, Helv. Chim. Acta 42 (1959) 1653.
[76] A.B. Sen, A.K. Sen Gupta, J. Indian Chem. Soc. 33 (1956) 437.
[77] S.S. Tiwari, B.N. Tripathi, J. Indian Chem. Soc. 33 (1956) 214.
[78] K. Reimer, Ber. Dtsch. Chem. Ges. 9 (1876) 423.
[79] K. Reimer, F. Tiemann, Ber. Dtsch. Chem. Ges. 9 (1876) 824.
[80] K. Reimer, F. Tiemann, Ber. Dtsch. Chem. Ges. 9 (1876) 1268.
[81] M. Mimuro, A. Murakami, Y. Fujita, Arch. Biochem. Biophys. 215 (1982) 266.
[82] W.H. Melhuish, J. Phys. Chem. 65 (1961) 229.
[83] A. Weller, Z. Elektrochem. 60 (1956) 1144.
[84] K.K. Smith, K.J. Kaufmann, J. Phys. Chem. 82 (1978) 2286.
[85] A. Mordziñski, K.H. Grellmann, J. Phys. Chem. 90 (1986) 5503.
[86] R. Englman, J. Jortner, Mol. Phys. 18 (1970) 145.
[87] N. Inamoto, Hammett Rule, Maruzen, Tokyo, 1983.
[88] C.D. Johnson, The Hammett Equation, Cambridge University Press, London, 1973.
[89] Y. Tsuno, M. Fujio, Chem. Soc. Rev. (1996) 129.
[90] I.B. Berlman, Handbook of Fluorescence Spectra of Aromatic Molecules, 2nd ed., Academic Press, New York, 1971.